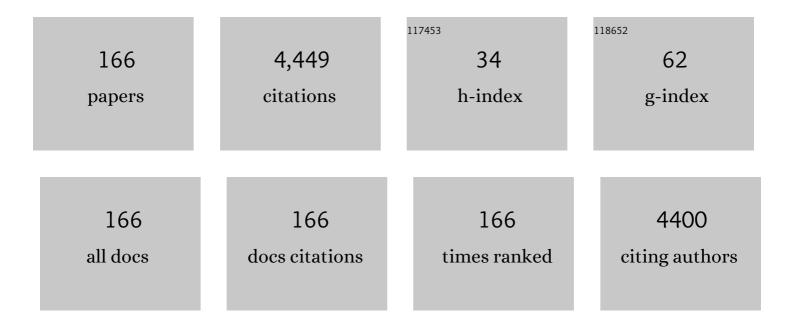
List of Publications by Year in descending order

Source: https://exaly.com/author-pdf/3442812/publications.pdf Version: 2024-02-01



#	Article	IF	CITATIONS
1	Ga-doped ZnO films grown on GaN templates by plasma-assisted molecular-beam epitaxy. Applied Physics Letters, 2000, 77, 3761-3763.	1.5	361
2	Layer-by-layer growth of ZnO epilayer on Al2O3(0001) by using a MgO buffer layer. Applied Physics Letters, 2000, 76, 559-561.	1.5	256
3	Stimulated emission and optical gain in ZnO epilayers grown by plasma-assisted molecular-beam epitaxy with buffers. Applied Physics Letters, 2001, 78, 1469-1471.	1.5	173
4	Origin of forward leakage current in GaN-based light-emitting devices. Applied Physics Letters, 2006, 89, 132117.	1.5	148
5	Synthesis of porous CuO nanowires and its application to hydrogen detection. Sensors and Actuators B: Chemical, 2010, 146, 266-272.	4.0	142
6	Band alignment at a ZnO/GaN (0001) heterointerface. Applied Physics Letters, 2001, 78, 3349-3351.	1.5	125
7	Investigation of ZnO epilayers grown under various Zn/O ratios by plasma-assisted molecular-beam epitaxy. Journal of Applied Physics, 2002, 92, 4354-4360.	1.1	122
8	Control of crystal polarity in a wurtzite crystal: ZnO films grown by plasma-assisted molecular-beam epitaxy on GaN. Physical Review B, 2002, 65, .	1.1	100
9	Origin of hexagonal-shaped etch pits formed in (0001) GaN films. Applied Physics Letters, 2000, 77, 82-84.	1.5	99
10	Plasma-assisted molecular-beam epitaxy of ZnO epilayers on atomically flat MgAl2O4(111) substrates. Applied Physics Letters, 2000, 76, 245-247.	1.5	98
11	Thermally activated deformation and the rate controlling mechanism in CoCrFeMnNi high entropy alloy. Materials Science & Engineering A: Structural Materials: Properties, Microstructure and Processing, 2017, 682, 569-576.	2.6	96
12	Structural and optical properties of non-polar A-plane ZnO films grown on R-plane sapphire substrates by plasma-assisted molecular-beam epitaxy. Journal of Crystal Growth, 2007, 309, 121-127.	0.7	90
13	Effects of an extremely thin buffer on heteroepitaxy with large lattice mismatch. Applied Physics Letters, 2001, 78, 3352-3354.	1.5	89
14	Co3O4–SWCNT composites for H2S gas sensor application. Sensors and Actuators B: Chemical, 2016, 222, 166-172.	4.0	75
15	Optimization of a zinc oxide urchin-like structure for high-performance gas sensing. Journal of Materials Chemistry, 2012, 22, 1127-1134.	6.7	73
16	Nanocomposite of cobalt oxide nanocrystals and single-walled carbon nanotubes for a gas sensor application. Sensors and Actuators B: Chemical, 2010, 150, 160-166.	4.0	68
17	Nanoheteroepitaxy of GaN on a nanopore array Si surface. Applied Physics Letters, 2003, 83, 1752-1754.	1.5	65
18	Control of polarity of ZnO films grown by plasma-assisted molecular-beam epitaxy: Zn- and O-polar ZnO films on Ga-polar GaN templates. Applied Physics Letters, 2000, 77, 3571-3573.	1.5	63

#	Article	IF	CITATIONS
19	ZnO epitaxial layers grown on c-sapphire substrate with MgO buffer by plasma-assisted molecular beam epitaxy (P-MBE). Semiconductor Science and Technology, 2005, 20, S13-S21.	1.0	62
20	Realization of an open space ensemble for nanowires: a strategy for the maximum response in resistive sensors. Journal of Materials Chemistry, 2012, 22, 6716.	6.7	60
21	Evaluation of nanopipes in MOCVD grown (0001) GaN/Al2O3 by wet chemical etching. Journal of Crystal Growth, 1998, 191, 275-278.	0.7	57
22	Morphology evolution of ZnO(000 1̄) surface during plasma-assisted molecular-beam epitaxy. Applied Physics Letters, 2002, 80, 1358-1360.	1.5	57
23	Formation and properties of self-organized Il–VI quantum islands. Thin Solid Films, 2000, 367, 68-74.	0.8	55
24	Low stacking-fault density in ZnSe epilayers directly grown on epi-ready GaAs substrates without GaAs buffer layers. Applied Physics Letters, 2001, 78, 165-167.	1.5	55
25	Enhancement of CO gas sensing properties in ZnO thin films deposited on self-assembled Au nanodots. Sensors and Actuators B: Chemical, 2010, 151, 127-132.	4.0	53
26	Influence of sputtering pressure on the microstructure evolution of AIN thin films prepared by reactive sputtering. Thin Solid Films, 1995, 261, 148-153.	0.8	52
27	Growth and structural properties of m-plane ZnO on MgO (001) by molecular beam epitaxy. Applied Physics Letters, 2008, 92, 233505.	1.5	51
28	Defect characterization in epitaxial ZnO/epi-GaN/Al2O3 heterostructures: transmission electron microscopy and triple-axis X-ray diffractometry. Journal of Crystal Growth, 2000, 209, 537-541.	0.7	47
29	Polarity control of ZnO films on (0001) Al2O3 by Cr-compound intermediate layers. Applied Physics Letters, 2007, 90, 201907.	1.5	45
30	Observation of ferromagnetism and anomalous Hall effect in laser-deposited chromium-doped indium tin oxide films. Solid State Communications, 2006, 137, 41-43.	0.9	44
31	Two-dimensional growth of ZnO films on sapphire(0001) with buffer layers. Journal of Crystal Growth, 2000, 214-215, 87-91.	0.7	42
32	Control of the ZnO Nanowires Nucleation Site Using Microfluidic Channels. Journal of Physical Chemistry B, 2006, 110, 3856-3859.	1.2	41
33	Polyaniline–chitosan nanocomposite: High performance hydrogen sensor from new principle. Sensors and Actuators B: Chemical, 2011, 160, 1020-1025.	4.0	40
34	A challenge in molecular beam epitaxy of ZnO: control of material properties by interface engineering. Thin Solid Films, 2002, 409, 153-160.	0.8	36
35	Plasma-assisted molecular beam epitaxy for ZnO based II–VI semiconductor oxides and their heterostructures. Journal of Vacuum Science & Technology an Official Journal of the American Vacuum Society B, Microelectronics Processing and Phenomena, 2000, 18, 1514.	1.6	34
36	Nanoscale modulated structures by balanced distribution of atoms and mechanical/structural stabilities in CoCuFeMnNi high entropy alloys. Materials Science & Engineering A: Structural Materials: Properties, Microstructure and Processing, 2019, 762, 138120.	2.6	34

#	Article	IF	CITATIONS
37	Enhanced Photoelectrochemical Activity of the TiO ₂ /ITO Nanocomposites Grown onto Singleâ€Walled Carbon Nanotubes at a Low Temperature by Nanocluster Deposition. Advanced Materials, 2011, 23, 5557-5562.	11.1	33
38	Anisotropic optical properties of free and bound excitons in highly strained A-plane ZnO investigated with polarized photoreflectance and photoluminescence spectroscopy. Applied Physics Letters, 2008, 92, 201907.	1.5	32
39	Growth and optical properties of ZnO nanorods prepared through hydrothermal growth followed by chemical vapor deposition. Journal of Alloys and Compounds, 2011, 509, 5137-5141.	2.8	32
40	ZnO and related materials: Plasma-Assisted molecular beam epitaxial growth, characterization and application. Journal of Electronic Materials, 2001, 30, 647-658.	1.0	31
41	Synthesis and hydrogen gas sensing properties of ZnO wirelike thin films. Journal of Vacuum Science and Technology A: Vacuum, Surfaces and Films, 2009, 27, 1347-1351.	0.9	31
42	Well-to-well non-uniformity in InGaN/GaN multiple quantum wells characterized by capacitance-voltage measurement with additional laser illumination. Applied Physics Letters, 2012, 100,	1.5	31
43	Evolution of initial layers of plasma-assisted MBE grown ZnO on (0001)GaN/sapphire. Journal of Crystal Growth, 2000, 214-215, 81-86.	0.7	30
44	Control and characterization of ZnO/GaN heterointerfaces in plasma-assisted MBE-grown ZnO films on GaN/Al2O3. Applied Surface Science, 2000, 159-160, 441-448.	3.1	30
45	Interface and defect structures in ZnO films on m-plane sapphire substrates. Journal of Crystal Growth, 2010, 312, 238-244.	0.7	30
46	High-Quality p-Type ZnO Films Grown by Co-Doping of N and Te on Zn-Face ZnO Substrates. Applied Physics Express, 2010, 3, 031103.	1.1	30
47	Effects of Basal Stacking Faults on Electrical Anisotropy of Nonpolar a-Plane (\$11ar{2}0\$) GaN Light-Emitting Diodes on Sapphire Substrate. IEEE Photonics Technology Letters, 2010, 22, 595-597.	1.3	29
48	ZnO epilayers on GaN templates: Polarity control and valence-band offset. Journal of Vacuum Science & Technology an Official Journal of the American Vacuum Society B, Microelectronics Processing and Phenomena, 2001, 19, 1429.	1.6	28
49	Strengthening and fracture of deformation-processed dual fcc-phase CoCrFeCuNi and CoCrFeCu1.71Ni high entropy alloys. Materials Science & Engineering A: Structural Materials: Properties, Microstructure and Processing, 2020, 781, 139241.	2.6	28
50	Characterization of microstructure and defects in epitaxial ZnO films on Al2O3 substrates by transmission electron microscopy. Journal of Crystal Growth, 2008, 310, 4102-4109.	0.7	26
51	Tin Oxide-Carbon Nanotube Composite for NO _{<i>X</i>} Sensing. Journal of Nanoscience and Nanotechnology, 2012, 12, 1425-1428.	0.9	26
52	Photoelectrochemical water splitting properties of hydrothermally-grown ZnO nanorods with controlled diameters. Electronic Materials Letters, 2015, 11, 65-72.	1.0	26
53	Improvement of Light Extraction Efficiency and Reduction of Leakage Current in GaN-Based LED Via V-Pit Formation. IEEE Photonics Technology Letters, 2012, 24, 449-451.	1.3	25
54	Study on MgO buffer in ZnO layers grown by plasma-assisted molecular beam epitaxy on Al2O3(0001). Thin Solid Films, 2003, 445, 213-218.	0.8	24

#	Article	IF	CITATIONS
55	Structural characteristics and magnetic properties of λ-MnO2 films grown by plasma-assisted molecular beam epitaxy. Journal of Applied Physics, 2001, 90, 351-354.	1.1	23
56	Nanostructural analysis of trabecular bone. Journal of Materials Science: Materials in Medicine, 2009, 20, 1419-1426.	1.7	23
57	Investigation of nonpolar (112Â ⁻ 0) a-plane ZnO films grown under various Zn/O ratios by plasma-assisted molecular beam epitaxy. Journal of Crystal Growth, 2010, 312, 2196-2200. Investigation of defect structure in homoepitaxial <mml:math< td=""><td>0.7</td><td>23</td></mml:math<>	0.7	23
58	xmlns:mml="http://www.w3.org/1998/Math/MathML" altimg="si1.svg"> <mml:mrow><mml:mo stretchy="true">(<mml:mrow><mml:mover) (accent="</td" 0="" 10="" 50="" 622="" etqq0="" overlock="" rgbt="" td="" tf="" tj=""><td>"true"><m 2.8</m </td><td>ml:mŋ>2</td></mml:mover)></mml:mrow></mml:mo </mml:mrow>	"true"> <m 2.8</m 	ml:mŋ>2
59	molecular beam epitaxy. Journal of Alloys and Compounds, 2020, 834, 155027. Reduction of dislocations in GaN films on AlN/sapphire templates using CrN nanoislands. Applied Physics Letters, 2008, 92, .	1.5	22
60	Precipitation and decomposition in CoCrFeMnNi high entropy alloy at intermediate temperatures under creep conditions. Materialia, 2019, 8, 100445.	1.3	22
61	Control of polarity of heteroepitaxial ZnO films by interface engineering. Applied Surface Science, 2002, 190, 491-497.	3.1	21
62	Self-separated freestanding GaN using a NH4Cl interlayer. Applied Physics Letters, 2007, 91, 192108.	1.5	21
63	Growth and structural properties of ZnO films on (10â^'10) m-plane sapphire substrates by plasma-assisted molecular beam epitaxy. Journal of Vacuum Science & Technology B, 2009, 27, 1625.	1.3	21
64	Improvement in crystallinity of ZnSe by inserting a low-temperature buffer layer between the ZnSe epilayer and the GaAs substrate. Journal of Crystal Growth, 2002, 242, 95-103.	0.7	20
65	ZnO nanowires prepared by hydrothermal growth followed by chemical vapor deposition for gas sensors. Journal of Vacuum Science & Technology B, 2009, 27, 1667-1672.	1.3	20
66	Three-Dimensional Hierarchical Structures of TiO ₂ /CdS Branched Core-Shell Nanorods as a High-Performance Photoelectrochemical Cell Electrode for Hydrogen Production. Journal of the Electrochemical Society, 2016, 163, H434-H439.	1.3	20
67	Growth and characterization of gallium oxide films grown with nitrogen by plasma-assisted molecular-beam epitaxy. Thin Solid Films, 2019, 682, 93-98.	0.8	19
68	Epitaxial Growth of Bandgap Tunable ZnSnN ₂ Films on (0001) Al ₂ O ₃ Substrates by Using a ZnO Buffer. Crystal Growth and Design, 2018, 18, 1385-1393.	1.4	18
69	Control of ZnO film polarity. Journal of Vacuum Science & Technology an Official Journal of the American Vacuum Society B, Microelectronics Processing and Phenomena, 2002, 20, 1656.	1.6	17
70	A Hydrogen Sulfide Gas Sensor Based on Pd-Decorated ZnO Nanorods. Journal of Nanoscience and Nanotechnology, 2016, 16, 10351-10355.	0.9	17
71	Effects of nanoepitaxial lateral overgrowth on growth of <i>α</i> -Ga2O3 by halide vapor phase epitaxy. Applied Physics Letters, 2019, 115, .	1.5	17
72	Origin of second-order nonlinear optical response of polarity-controlled ZnO films. Applied Physics Letters, 2009, 94, .	1.5	16

#	Article	IF	CITATIONS
73	Highly Asymmetric Optical Properties of β-Ga ₂ O ₃ as Probed by Linear and Nonlinear Optical Excitation Spectroscopy. Journal of Physical Chemistry C, 2021, 125, 1432-1440.	1.5	16
74	Properties of (11–20) a-plane ZnO films on sapphire substrates grown at different temperatures by plasma-assisted molecular beam epitaxy. Thin Solid Films, 2011, 519, 6394-6398.	0.8	15
75	Microstructural degradation during Zn diffusion in a GalnAsP/InP heterostructure: Layer mixing, misfit dislocation generation, and Zn3P2precipitation. Journal of Applied Physics, 1992, 72, 4063-4072.	1.1	14
76	Nanostructure formation and emission characterization of blue emission InN/GaN quantum well with thin InN well layers. Journal of Crystal Growth, 2005, 281, 349-354.	0.7	14
77	Growth of Polarity-Controlled ZnO Films on (0001) Al2O3. Journal of Electronic Materials, 2008, 37, 736-742.	1.0	14
78	Magneto-transport properties of amorphous Ge1â^'xMnx thin films. Current Applied Physics, 2006, 6, 545-548.	1.1	13
79	Effect of indium concentration on morphology of ZnO nanostructures grown by using CVD method and their application for H2 gas sensing. Superlattices and Microstructures, 2015, 82, 349-356.	1.4	13
80	Microstructural Investigation of CoCrFeMnNi High Entropy Alloy Oxynitride Films Prepared by Sputtering Using an Air Gas. Metals and Materials International, 2018, 24, 1285-1292.	1.8	13
81	Effects of low temperature ZnO and MgO buffer thicknesses on properties of ZnO films grown on (0001) Al2O3 substrates by plasma-assisted molecular beam epitaxy. Thin Solid Films, 2010, 519, 223-227.	0.8	12
82	Effects of growth pressure on morphology of ZnO nanostructures by chemical vapor transport. Chemical Physics Letters, 2016, 658, 182-187.	1.2	12
83	Magnetic and electrical properties of MBE-grown (Ge1â^'xSix)1â^'yMny thin films. Current Applied Physics, 2006, 6, 478-481.	1.1	11
84	Interface Engineering in ZnO Epitaxy. Physica Status Solidi (B): Basic Research, 2002, 229, 803-813.	0.7	10
85	Structural and optical investigations of periodically polarity inverted ZnO heterostructures on (0001) Al2O3. Applied Physics Letters, 2009, 94, 141904.	1.5	10
86	Ultrastructural observation of electron irradiation damage of lamellar bone. Journal of Materials Science: Materials in Medicine, 2009, 20, 959-965.	1.7	10
87	Raman and emission characteristics of a-plane InGaN/GaN blue-green light emitting diodes on r-sapphire substrates. Journal of Applied Physics, 2011, 109, 043103-043103-4.	1.1	10
88	Growth of single crystal non-polar (<mml:math)="" etqq0<="" td="" tj="" xmlns:mml="http://www.w3.org/1998/Math/MathML"><td>0 0 rgBT /0 3.1</td><td>Overlock 10 T 10</td></mml:math>	0 0 rgBT /0 3.1	Overlock 10 T 10
89	sapphire substrate. Applied Surface Science, 2019, 481, 819-824. Growth and Characterization of Zinc Oxide Nanostructures on (111) Silicon Substrates with Aluminum Compound Layer. Journal of the Korean Physical Society, 2008, 53, 292-298.	0.3	10
90	Doping effects in ZnO layers using Li3N as a doping source. Journal of Crystal Growth, 2003, 251, 628-632.	0.7	9

#	Article	IF	CITATIONS
91	Investigation of initial growth and very thin () ZnO films by cross-sectional and plan-view transmission electron microscopy. Applied Surface Science, 2010, 256, 1849-1854.	3.1	9
92	Reduction of dislocations in α-Ga ₂ O ₃ epilayers grown by halide vapor-phase epitaxy on a conical frustum-patterned sapphire substrate. IUCrJ, 2021, 8, 462-467.	1.0	9
93	Control of crystal polarity in oxide and nitride semiconductors by interface engineering. Journal of Electroceramics, 2006, 17, 255-261.	0.8	8
94	Experimental verification of effects of barrier dopings on the internal electric fields and the band structure in InGaN/GaN light emitting diodes. Applied Physics Letters, 2014, 104, .	1.5	8
95	Growth and Characterization of Zinc-Oxide Films Grown by Using Plasma-Assisted Molecular Beam Epitaxy on (111) Silicon Substrates with Ti and Titanium Compound Buffer Layers. Journal of the Korean Physical Society, 2008, 53, 276-281.	0.3	8
96	Structural investigation of nitrided c-sapphire substrate by grazing incidence x-ray diffraction and transmission electron microscopy. Applied Physics Letters, 2007, 91, 202116.	1.5	7
97	The roles of low-temperature buffer layer for thick GaN growth on sapphire. Journal of Crystal Growth, 2008, 310, 920-923.	0.7	7
98	Effects of Zn pre-exposure temperature on the microstructures of ZnO films grown on Si(001) substrates by plasma-assisted molecular beam epitaxy. Journal of Crystal Growth, 2008, 310, 1118-1123.	0.7	6
99	Effects of two-step growth by employing Zn-rich and O-rich growth conditions on properties of (1120) ZnO films grown by plasma-assisted molecular beam epitaxy on sapphire. Journal of Vacuum Science & Technology B, 2009, 27, 1635.	1.3	6
100	Lateral arrays of vertical ZnO nanowalls on a periodically polarity-inverted ZnO template. Nanotechnology, 2009, 20, 235304.	1.3	6
101	Electrical and magnetic properties of Mn-doped Si thin films. Physica B: Condensed Matter, 2009, 404, 1686-1688.	1.3	6
102	Effects of strainâ€control layers on piezoelectric field and indium incorporation in InGaN/GaN blue quantum wells. Physica Status Solidi - Rapid Research Letters, 2010, 4, 221-223.	1.2	6
103	A simple fabrication method of randomly oriented polycrystalline zinc oxide nanowires and their application to gas sensing. Advances in Natural Sciences: Nanoscience and Nanotechnology, 2011, 2, 015002.	0.7	6
104	Lattice Deformation in \$a\$-Plane ZnO Films Grown on \$r\$-Plane Al\$_{2}\$O\$_{3}\$ Substrates Grown by Plasma-Assisted Molecular-Beam Epitaxy. Applied Physics Express, 2012, 5, 081101.	1.1	6
105	Ferromagnetism and Anomalous Hall Effect in p-Zn0.99Mn0.01O:P. Journal of Magnetics, 2005, 10, 95-98.	0.2	6
106	Influence of growth flux and surface supersaturation on InGaAs/GaAs strain relaxation. Applied Physics Letters, 2004, 84, 1085-1087.	1.5	5
107	Growth and magnetism in amorphous Si1â^'xMnx thin films grown by thermal deposition. Journal of Magnetism and Magnetic Materials, 2006, 304, e167-e169.	1.0	5
108	Spontaneous transition in preferred orientation of GaN domains grown on r-plane sapphire substrate from [112Â ⁻ 0] to [0001]. Applied Physics Letters, 2009, 94, 102103.	1.5	5

#	Article	IF	CITATIONS
109	Hydride vapor phase epitaxy of GaN on the vicinal c-sapphire with a CrN interlayer. Journal of Crystal Growth, 2009, 311, 470-473.	0.7	5
110	Microstructural Analysis of Void Formation Due to a NH4Cl Layer for Self-Separation of GaN Thick Films. Crystal Growth and Design, 2009, 9, 2877-2880.	1.4	5
111	Structural and stimulated emission characteristics of diameter-controlled ZnO nanowires using buffer structure. Journal Physics D: Applied Physics, 2009, 42, 225403.	1.3	5
112	Microstructural investigation of ZnO films grown on (111) Si substrates by plasma-assisted molecular beam epitaxy. Journal of Crystal Growth, 2010, 312, 1557-1562.	0.7	5
113	Transparent Nanoscale Floating Gate Memory Using Selfâ€Assembled Bismuth Nanocrystals in Bi ₂ Mg _{2/3} Nb _{4/3} O ₇ (BMN) Pyrochlore Thin Films Grown at Room Temperature. Advanced Materials, 2012, 24, 3396-3400.	11.1	5
114	Heteroepitaxial growth of GaN on various powder compounds (AlN, LaN, TiN, NbN, ZrN, ZrB 2 , VN, BeO) by hydride vapor phase epitaxy. Electronic Materials Letters, 2012, 8, 135-139.	1.0	5
115	In Situ Oxidation of GaN Layer and Its Effect on Structural Properties of Ga2O3 Films Grown by Plasma-Assisted Molecular Beam Epitaxy. Journal of Electronic Materials, 2017, 46, 3499-3506.	1.0	5
116	Comprehensive study of the surface morphology evolution induced by thermal annealing in single-crystalline ZnO Films and ZnO bulks. Journal of the Korean Physical Society, 2012, 61, 1732-1736.	0.3	4
117	Microstructural Characterization of High Indium-Composition InXGa1â^'XN Epilayers Grown on c-Plane Sapphire Substrates. Microscopy and Microanalysis, 2013, 19, 145-148.	0.2	4
118	Crystal orientation variation of nonpolar AlN films with III/V ratio on r-plane sapphire substrates by plasma-assisted molecular beam epitaxy. Electronic Materials Letters, 2014, 10, 1109-1114.	1.0	4
119	Growth and characterization of Mg Zn1â^'O films grown on r-plane sapphire substrates by plasma-assisted molecular beam epitaxy. Journal of Alloys and Compounds, 2015, 623, 1-6.	2.8	4
120	Depth dependent strain analysis in GaN-based light emitting diodes using surface-plasmon enhanced Raman spectroscopy. Physica Status Solidi (A) Applications and Materials Science, 2017, 214, 1600805.	0.8	4
121	Determination of defect types of ZnSe-based epilayers by etch-pit configurations. Journal of Crystal Growth, 1997, 181, 343-350.	0.7	3
122	Characterization of ZnSe/ZnMgBeSe single quantum wells. Physica E: Low-Dimensional Systems and Nanostructures, 2000, 7, 576-580.	1.3	3
123	Slowdown in development of self-assembled InAsâ^•GaAs(001) dots near the critical thickness. Journal of Vacuum Science & Technology B, 2006, 24, 1886.	1.3	3
124	Growth of epitaxial ZnO films on Si (1 1 1) substrates with Cr compound buffer layer by plasma-assisted molecular beam epitaxy. Journal of Crystal Growth, 2010, 312, 2190-2195.	0.7	3
125	Effects of gallium doping on properties of a-plane ZnO films on r-plane sapphire substrates by plasma-assisted molecular beam epitaxy. Journal of Vacuum Science and Technology A: Vacuum, Surfaces and Films, 2011, 29, 03A111.	0.9	3
126	Comprehensive Study about the Effect of Heat Treatment on the Electrical Properties of Single-Crystalline ZnO Materials. Applied Physics Express, 2012, 5, 075801.	1.1	3

#	Article	IF	CITATIONS
127	Investigation of the photoelectrochemical properties for typical ZnO nanostructures grown by using chemical vapor transport. Journal of the Korean Physical Society, 2015, 66, 832-838.	0.3	3
128	Non-alloyed Au/p-ZnSe/p-BeTe ohmic contact layers for ZnSe-based blue-green laser diodes. Electronics Letters, 1999, 35, 1740.	0.5	3
129	Temperature and Polarization Dependence of the Near-Band-Edge Photoluminescence in a Non-Polar ZnO Film Grownby Using Molecular Beam Epitaxy. Journal of the Korean Physical Society, 2008, 53, 288-291.	0.3	3
130	Fabrication and Photoelectrochemical Properties of a Cu2O/CuO Heterojunction Photoelectrode for Hydrogen Production from Solar Water Splitting. Korean Journal of Materials Research, 2016, 26, 604-610.	0.1	3
131	Correlation of surface chemistry of GaAs substrates with growth mode and stacking fault density in ZnSe epilayers. Journal of Vacuum Science and Technology A: Vacuum, Surfaces and Films, 2002, 20, 1948.	0.9	2
132	Dynamic Characteristics of Metal-Induced Laterally Crystallized Polycrystalline Silicon Thin-Film Transistor Devices and Circuits Fabricated with Asymmetric Precrystallization. Japanese Journal of Applied Physics, 2009, 48, 020205.	0.8	2
133	Growth and optical properties of ZnO nanorods prepared through hydrothermal growth followed by chemical vapor deposition. , 2010, , .		2
134	Anisotropic properties of periodically polarity-inverted zinc oxide structures. Journal of Applied Physics, 2010, 107, 123519.	1.1	2
135	The thermal treatment effects of CrN buffer layer on crystal quality of Zn-polar ZnO films. Thin Solid Films, 2011, 519, 3417-3420.	0.8	2
136	Surface Polarity Effects on the Hydride Vapor Phase Epitaxial Growth of GaN on 6H-SiC with a Chrome Nitride Buffer Layer. Electrochemical and Solid-State Letters, 2012, 15, H148.	2.2	2
137	Hydrothermal Synthesis of ZnO Nanorods in the Presence of a Surfactant. Journal of Nanoscience and Nanotechnology, 2012, 12, 1328-1331.	0.9	2
138	Growth and stuctural characterization of InGaN layers with controlled In content prepared by plasma-assisted molecular beam epitaxy. Thin Solid Films, 2013, 546, 42-47.	0.8	2
139	High Temperature Behavior of Injection and Radiative Efficiencies and Its Effects on the Efficiency Droop in InGaN/GaN Light Emitting Diodes. Journal of Nanoscience and Nanotechnology, 2016, 16, 11640-11644.	0.9	2
140	Strain mapping in a nanoscale-triangular SiGe pattern by dark-field electron holography with medium magnification mode. Microscopy (Oxford, England), 2016, 65, 499-507.	0.7	2
141	Comprehensive Study of the Surface Morphology Evolution Induced by Thermal Annealing in <i>A</i> -Plane ZnO Films on <i>R</i> -Plane Al ₂ O ₃ Substrates. Science of Advanced Materials, 2016, 8, 358-362.	0.1	2
142	Dynamic Characteristics of Multi-Channel Metal-Induced Unilaterally Precrystallized Polycrystalline Silicon Thin-FilmTransistor Devices and Circuits. Korean Journal of Materials Research, 2008, 18, 507~510-507~510.	0.1	2
143	Growth of Epitaxial AlN Thin Films on Sapphire Substrates by Plasma-Assisted Molecular Beam Epitaxy. Korean Journal of Materials Research, 2011, 21, 634-638.	0.1	2
144	Systematic Investigation of Growth and Properties of Ga ₂ O ₃ Films on C-Plane Sapphire Substrates Prepared by Plasma-Assisted Molecular Beam Epitaxy. ECS Journal of Solid State Science and Technology, 2022, 11, 035008.	0.9	2

#	Article	IF	CITATIONS
145	2D strain measurement in sub-10Ânm SiGe layer with dark-field electron holography. Current Applied Physics, 2015, 15, 1529-1533.	1.1	1
146	Simultaneous determination of defect distributions and energies near InGaN/GaN quantum wells by capacitance–voltage measurement. Journal Physics D: Applied Physics, 2017, 50, 39LT03.	1.3	1
147	Effect of in situ annealing on the structural properties of Bi2Te3 films grown on (0â€0â€0â€1) sapphire. Journal of Crystal Growth, 2019, 525, 125191.	0.7	1
148	Effect of First-Stage Growth Manipulation and Polarity of SiC Substrates on AlN Epilayers Grown Using Plasma-Assisted Molecular Beam Epitaxy. Korean Journal of Materials Research, 2014, 24, 266~270-266~270.	0.1	1
149	Structural Characterization of CoCrFeMnNi High Entropy Alloy Oxynitride Thin Film Grown by Sputtering. Korean Journal of Materials Research, 2018, 28, 595-600.	0.1	1
150	Plasma-Assisted Molecular-Beam Epitaxy of ZnO Films on (0001) Al2O3: Effects of the MgO Buffer Layer Thickness. Journal of the Korean Physical Society, 2008, 53, 271-275.	0.3	1
151	Structural and Optical Properties of ZnO Thin Films Grown on SiO2/Si(100) Substrates by RF Magnetron Sputtering. Korean Journal of Materials Research, 2006, 16, 360-366.	0.1	1
152	Effects of Growth Rate and III/V Ratio on Properties of AlN Films Grown on c-Plane Sapphire Substrates by Plasma-Assisted Molecular Beam Epitaxy. Korean Journal of Materials Research, 2019, 29, 579-585.	0.1	1
153	Ferromagnetism and anomalous Hall effect in Mn-doped ZnO thin films grown by reactive sputtering. , 2005, , .		0
154	The Growth of ZnO on CrN Buffer Layer Using Surface Phase Control by Plasma Assisted Molecular-beam Epitaxy. Materials Research Society Symposia Proceedings, 2006, 957, 1.	0.1	0
155	Strong enhancement of emissions from nanostructured ZnO thin films grown by plasmaâ€assisted molecularâ€beam epitaxy on nanopored Si(001) substrates. Physica Status Solidi (A) Applications and Materials Science, 2008, 205, 1598-1601.	0.8	0
156	Investigations on growth and hydrogen gas sensing property of ZnO nanowires prepared by hydrothermal growth. , 2010, , .		0
157	Growth of self-standing GaN substrates. , 2010, , .		0
158	NO gas sensing properties of ZnO wire-like thin films synthesized by thermal oxidation of sputtered Zn metallic films in air. , 2010, , .		0
159	Suppression of composition modulation in Inâ€rich In _{<i>x</i>} Ga _{1â^²<i>x</i>} N layer with high In content (<i>x</i> â^¼â€‰0.67). Physica Status Solidi (A) Applications and Materials Scien 2011, 208, 2737-2740.	C @. 8	0
160	Selected Peer-Reviewed Articles from the International Union of Materials Research Societies—International Conference on Electronic Materials 2010 (IUMRS-ICEM 2010). Journal of Nanoscience and Nanotechnology, 2012, 12, 1128-1130.	0.9	0
161	Effect of Refined Nitridation of Sapphire Substrates in Hydride Vapor Phase Epitaxy: Definite Correlation of Structural Characteristics between a Low-Temperature-Grown Buffer Layer and a Subsequent High-Temperature-Grown Layer of GaN. Journal of the Korean Physical Society, 2009, 54, 2404-2408.	0.3	0
162	Structural Characterization of Bismuth Zinc Oxide Thin Films Grown by Plasma-Assisted Molecular Beam Epitaxy. Korean Journal of Materials Research, 2011, 21, 563-567.	0.1	0

#	Article	IF	CITATIONS
163	Plasma-Assisted Molecular Beam Epitaxy of InXGa1-XN Films on C-plane Sapphire Substrates. Korean Journal of Materials Research, 2012, 22, 185-189.	0.1	Ο
164	Growth Characteristics of AlN by Plasma-Assisted Molecular Beam Epitaxy with Different Al Flux. Korean Journal of Materials Research, 2012, 22, 539-544.	0.1	0
165	Comprehensive Structural Characterization of Commercial Blue Light Emitting Diode by Using High-Angle Annular Dark Filed Scanning Transmission Electron Microscopy and Transmission Electron Microscopy. Korean Journal of Materials Research, 2015, 25, 1-8.	0.1	0
166	Characterization of Basal Plane Dislocations in PVT-Grown SiC by Transmission Electron Microscopy. Korean Journal of Materials Research, 2016, 26, 656-661.	0.1	0